

D.V. Mann

7.1 Introduction

The selection and timing of management options for cholangiocarcinoma must necessarily be informed by the function of the liver. The consideration of major resectional hepatic surgery is predicated on the ability of that organ to sustain and recover adequate hepatocyte function and mass, whereas individuals presenting with biliary obstruction may benefit from axial or segmental restoration of bile egress prior to planned therapy. Assessment of liver physiological status therefore guides treatment options for cholangiocarcinoma whether arising in the extrahepatic or intrahepatic components of the biliary system. Ideally, an evaluation of liver function should assess not only ambient homeostatic performance but also the recuperative and regenerative capacity of that organ (the functional reserve) since these restorative processes are less efficient in the severely parenchymal-depleted, diseased or cholestatic state [1, 2]. It should be appreciated however, that when the malignant process is confined to one hemi-liver (or segmental components) there may be no measurable disturbance in serum biochemistry or test-substance handling due to compensation by the unaffected liver, and in this situation techniques that assess hepatocyte status per se may be more informative. In addition to those estimations used for initial evaluation prior to planned therapy, serial or longitudinal studies can be used to monitor hepatic status after intervention and to detect deviation from expected patterns of recovery before these become clinically manifest.

The term liver function encompasses a whole host of the biologic roles of that organ including not only diverse metabolic tasks, but also the physiological response to injury (acute phase reaction) and capability for restoration of lost liver mass (regeneration). Although many of the commonly used traditional peripheral blood “liver function tests” do not

directly measure actual function, and changes in most are not specific to that organ, these analyses (particularly in combination) have generally proven robust in the prediction of outcomes following hepatectomy [3]. Estimations of liver volume are often used to predict physiological capacity and reserve. However, parenchymal mass and function may be dissociated in the diseased or regenerating condition and therefore probing of some other dimension of hepatic performance may be desirable for more complete representation.

The assessment of liver physiology can be considered according to the following conceptual framework of four main types of test (Table 7.1):

1. Homeostatic: traditional “liver function tests”; biochemical analyses of blood reflecting the balance between production and disappearance of bile metabolites, hepatic enzymes and plasma proteins. These may be combined with clinical evaluations to produce composite clinico-biochemical scoring systems (e.g., Child-Pugh grading)
2. Radiological: image based assessments of liver parenchymal volume and quality;

Table 7.1 Taxonomy of liver function tests

Type	Examples
Homeostatic	Bilirubin Transaminases Alkaline phosphatase Albumin Prothrombin time Clinico-laboratory scoring (e.g., Child-Pugh score)
Radiological	Computer tomography volumetry Hepatic steatosis measurement
Bioenergetic	Redox state Adenine nucleotide/mitochondrial analysis Magnetic resonance spectroscopy
Dynamic	Clearance tests e.g., indocyanine green, aminopyrine, MEGX Hexose sugar handling capacity Hepatic scintigraphy Portal vein embolization

D.V. Mann, MS, FRCS
8/F Hang Wai Building, 231 Queens Road East,
Wanchai, Hong Kong
e-mail: darrenmann@biznetvigator.com

3. Bioenergetic: measures of hepatic energy state (in plasma and at tissue level);
4. Dynamic tests: in which some aspect of liver physiology is assessed in a time dependent manner (e.g., tracer excretion) or repeated measures of any of the above tests used to assess the longitudinal response to a provocation such as metabolic stress or portal vein embolization.

This chapter will describe these tests, with greatest emphasis on those that have become clinically established in the management of patients with cholangiocarcinoma. Emerging technologies poised to contribute to clinical advancements in the future or that provide new insights with which to interpret currently used tests will also be discussed.

7.2 Homeostasis

The term liver function is used to describe the diverse biological duties of that organ, which include intermediary metabolism of carbohydrates, protein and fat, production of bile, synthesis of plasma proteins and clotting factors, metabolic handling and excretion of endo- and xenobiotics and urea synthesis. In addition, the cellular integrity of hepatocytes and bile canaliculi can be inferred from circulating levels of enzymes normally confined to the intracellular domain. A common biochemical panel of “liver function tests” comprises estimation of the serum level of bilirubin, transaminases, alkaline phosphatase, albumin level and clotting factor analysis. Each of these elements is reflective of a different element of liver physiology and its disorder.

7.2.1 Bilirubin

The plasma concentration of the chemical tetrapyrrole bilirubin, the main degradation product of heme-protein metabolism, reflects the aggregate processes of production by the reticulo-endothelial system, and subsequent hepatic extraction, conjugation and excretion by an active anionic transport mechanism. When rate of generation is constant, the circulating level is taken to represent overall bile pigment “handling” by the liver. However, bilirubin levels may be influenced by non-hepatic factors, for example increased production by haemolysis and sepsis, and decreased clearance due to mechanical obstruction to bile flow, and therefore may not reflect hepatocyte function per se in these instances. Although independently predictive of morbidity following hepatic resection [4], plasma bilirubin concentration is most commonly combined with other laboratory and clinical factors such as Child-Pugh scoring system or Model for End-stage Liver Disease (MELD) (see below). A pattern of progressive increase in bilirubin after liver resection may

herald the onset of organ dysfunction, although sepsis, drug reaction, biliary obstruction and portal vein thrombosis may also present in this way.

7.2.2 Transaminases

Serum activities of amino-transferase enzymes are reflective of hepatic cellular integrity, although specificity may be reduced by contributions from other organs, particularly striated muscle. Alanine transferase (ALT) is purely cytosolic in origin (and more specific), whilst aspartate transferase (AST) is of mixed mitochondrial and cytosolic provenance (and more sensitive). Elevated preoperative transaminase levels have been found to be associated with increased risk of complications and death after liver resection in cirrhotic patients [5]. A markedly elevated transaminase level is suggestive of ongoing hepatic necrosis, for example active viral or alcoholic hepatitis, ischemia or sepsis (particularly of biliary tract). The relative weighting of these enzymes for risk is comparatively weak, and they do not routinely feature in composite preoperative scores.

7.2.3 Alkaline Phosphatase

Alkaline phosphatases are a group of hydrolase enzymes responsible for removing phosphate groups in the 5- and 3-positions from many types of molecules, including nucleotides, proteins, and alkaloids. They are distributed in liver, bile ducts, bone, kidney and placenta. Hepatic-origin alkaline phosphatase levels are elevated in the presence of liver disease with hepatic cell injury or biliary obstruction, mechanistically due to increased enzyme synthesis as well as plasma spill-over. Preoperative serum activity of alkaline phosphatase may be predictive of risk of hepatic failure following hepatectomy [6]. Liver regeneration following hepatectomy is associated with an elevation of alkaline phosphatase levels, and failure of regeneration may be presaged when levels of this enzyme do not increase in the post-hepatectomy period.

7.2.4 Albumin

This plasma protein is synthesized exclusively by the liver. The circulating half-life is 20 days, and assay can be used to interpret steady state synthetic function (although starvation and protein losing conditions also influence levels). An acute reduction in plasma concentration more likely reflects change in volume of distribution due to capillary leakage rather than diminished synthesis. Albumin has prognostic value for risk of liver surgery as part of the Child-Pugh score.

Table 7.2 Child-Pugh score

Measure	1 point	2 points	3 points	Units
Bilirubin (total)	<34 (<2)	34–50 (2–3)	>50 (>3)	umol/l (mg/dL)
Serum albumin	>35	28–35	<28	g/L
INR	<1.7	1.71–2.20	>2.20	No unit
Ascites	None	Suppressed with medication	Refractory	No unit
Hepatic encephalopathy	None	Grade I–II (or suppressed with medication)	Grade III–IV (or refractory)	No unit

7.2.5 Prothrombin Time

The liver is the predominant site for the manufacture of blood clotting cascade proteins. Derangements in liver function may therefore be detected by disturbed laboratory measures of clotting times, or reduced amounts of individually assayed clotting factors. The commonest measurement is that of prothrombin time, which is indicative of the extrinsic pathway of coagulation involving factors II, V, VII, X and fibrinogen. The prothrombin time is predominantly affected by factor VII which has the shortest half life (4–6 h) and is vitamin K dependent (so abnormalities may arise from vitamin K insufficiency states such as biliary obstruction as well as protein-synthetic deficits). Prothrombin time is a component of the Child-Pugh score.

7.2.6 Prognostic Clinico-Laboratory Scoring

A common method for evaluation of hepatic function is the use of a composite prognostication system based on laboratory measures and selected clinical criteria. These components reflect different core aspects of liver physiology including endobiotic handling and excretion, protein synthesis and clinical estimates of degree of established portal hypertension, which can be combined into an overall score. In general the scores are formulated by multivariate logistic regression methods, and the advantage is that a greater degree of overall liver function is represented (parallel testing enhances sensitivity) and the predictive power goes beyond that of any individual component test. Although initially devised for risk assessment in the setting of liver cirrhosis, the use of scoring systems is often extended in clinical practice to evaluate suitability for liver surgery in general. Such scores are predictive of natural history of liver disease, and may stratify risk of therapeutic interventions and prioritise selection for transplantation.

7.2.6.1 The Child-Pugh Score

The Child score (Pugh modification) is the most widely used system and is composed of bilirubin (excretion), albumin (synthetic function), prothrombin time (synthesis), ascites (portal hypertension) and encephalopathy (porto-systemic shunting) [7]. Components of the system and point

allocation for scoring are shown in Table 7.2. Individuals are grouped onto Classes according to the number of points, as follows: Class A 5–6; Class B 7–9 and Class C 10–15 (there is some variation in the literature between authors on Class allocation). Since cholangiocarcinoma (and mixed cholangio-hepatocellular carcinoma) may occasionally arise in the setting of pre-existing liver disease, the Child-Pugh score is commonly used to evaluate operative risk. In particular, the outcomes of liver resectional surgery are numerically related to Child-Pugh score, with mortality rates being lower and survival rates higher in Child-Pugh Class A compared to Class B and C [8, 9]. Child-Pugh Class A, well-compensated cirrhosis, does not negatively impact on survival after hepatectomy [10].

7.2.6.2 Model for End-Stage Liver Disease (MELD)

The MELD score is a commonly used to rank patients for liver transplantation, and is mentioned here because this is a therapeutic option that can be selectively considered in the management of cholangiocarcinoma [11]. Scores are calculated according to the formula: $MELD = 0.957 \times \log e(\text{creatinine mg/dl}) + 0.378 \times \log e(\text{bilirubin mg/dl}) + 1.120 \log e(\text{INR}) + 0.643$.

MELD has been examined as an alternative to Child-Pugh score for prediction of liver failure post hepatectomy. Although MELD score is correlated with risk of liver failure after resection, it is unclear whether the discriminant function is superior to Child-Pugh Class [3, 12].

7.3 Radiological Imaging and Qualitative Assessments

Volumetric analysis of the liver parenchyma forms an integral component of the assessment of functioning liver cell mass, and by extension predicted physiological reserve. Computed tomography liver volumetry can be used to assess the respective volumes of liver and tumour, and to estimate the parenchymal resection rate and so judge the suitability for resectional surgery [13, 14]. Estimates of postoperative liver volume can be used to guide selection of therapies for cholangiocarcinoma, in the context of the condition of the underlying liver [15]. For example, when inadequate post-operative parenchymal volume is anticipated, measures to

increase hepatic cell mass such as portal vein embolization may be indicated, or non-resectional alternatives (transplantation, chemo-irradiation, local ablation, etc.) considered.

Volumetric estimations can be combined with functional analyses such as indocyanine green retention (see below) to provide composite scores of high accuracy for predicting complications and outcomes of liver surgery [16].

Hepatic steatosis (fatty liver) is a risk factor for complications and death after liver resection, and some authors advocate pre-operative identification prior to major hepatic resection: the fat content of the liver can be assessed by ultrasound, computed tomography or magnetic resonance imaging [17].

7.4 Bioenergetic Tests

The traditional liver function tests outlined above are used to identify disturbance in several of the possible biologic roles of the liver. However, results may be influenced by diverse non-hepatic factors and there is often variation in the degree of perturbation of different tests. A limitation common to these evaluations is that they are indirectly reflective of underlying liver physiology. Although these tests can be augmented by liver volumetry, it should be appreciated that in the diseased state there may be a dissociation between hepatocyte mass and performance, and therefore volumetric indices may not accurately reflect functional reserve. Conversely, serum biochemistry may be misleadingly normal in certain disease states, for example a biliary obstructed hemi-liver, due to compensatory processes. Because of these limitations, estimations of organ energy balance have intrinsic appeal since they may more reliably reflect the condition of hepatocytes.

Fundamentally, the key determinant of hepatic functional status and reserve is the energy state of the organ, which in

turn is determined by the aggregate energy balance of individual hepatocytes. Energy transduction for maintenance of cellular integrity and function is achieved through the adenylate high-energy phosphate system, the principal mediator being adenosine triphosphate (ATP). In the liver, each individual hepatocyte may be considered as a self-recharging battery in which energy status is controlled according to energy charge $(ATP + 1/2ADP)/(ATP + ADP + AMP)$ or phosphorylation potential $(ATP/ADP \times Pi)$ [18]. These key metabolic parameters govern the balance between energy-producing (exergonic) and energy-consuming (endergonic) processes, thereby maintaining the biochemical poise of the system.

A fall in energy state induces a curtailment of synthetic, secretory and storage reactions, while favouring energy-producing ones (and vice versa) thereby tending to restore equipoise when energy demands and supply (temporarily) dissociate (Fig. 7.1). When net energy consumption exceeds supply, whether due to increased physiologic demands or to limitations of ATP-generating ability secondary to disease (or some combination of the two) then a fall in energy state is produced. By the action of feedback modification, a compensatory suppression of ATP-consuming processes will result. This has widespread and varied consequences for liver function, but not all aspects of hepatocyte biology will necessarily be affected to the same degree for any given magnitude of energy state depression (Fig. 7.2 shows schematically the physiologic consequences of energy balance deficit after liver resection). Active anionic transport and protein synthesis are typical of energy-consuming processes that are curtailed during conditions of energy state depression, hence plasma bilirubin levels tend to rise and prothrombin and albumin levels fall. Other important energy-dependent processes such as nucleic acid synthesis may also be suppressed with important implications for mitotic capacity and regeneration. More extreme deviations

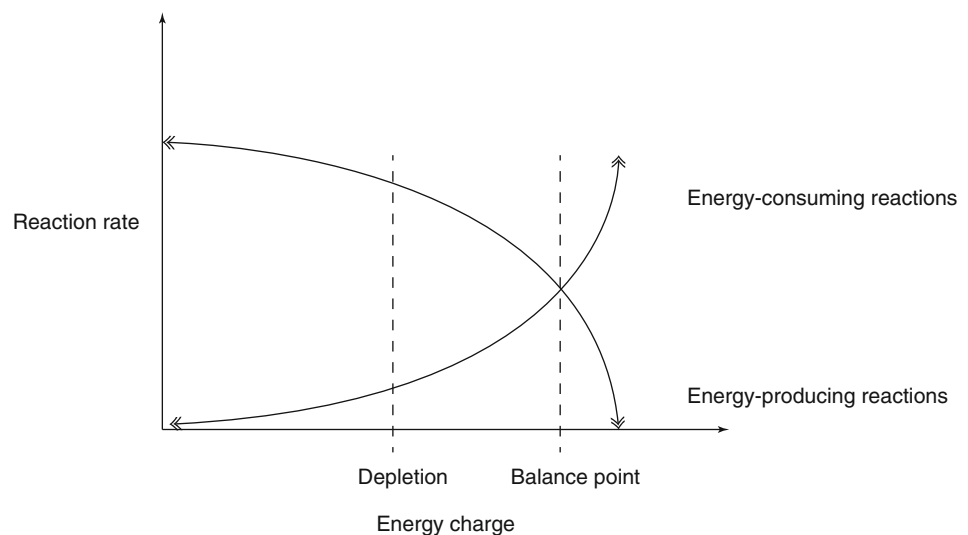
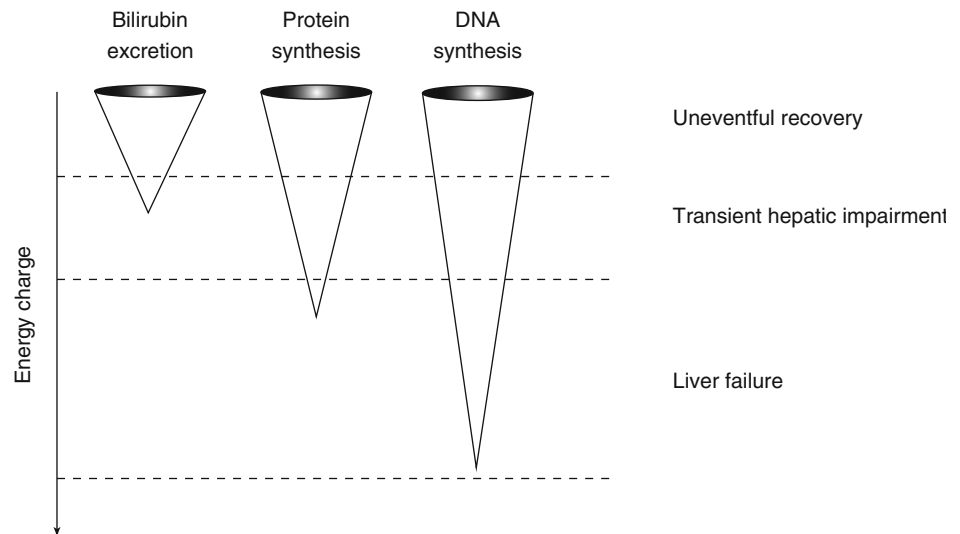


Fig. 7.1 Energy charge and metabolic control. The graph shows how a reduction in energy state at 'depletion' results in a decrease in energy-consuming reaction rates (secretion, synthesis, storage) and increase in energy-producing reaction rates, thereby restoring the system to the energy "balance point"

Fig. 7.2 Energy state and liver function after liver resectional surgery. A fall in hepatic energy charge necessarily results in some limitation of energy-consuming processes such as those for excretion of bilirubin, production of proteins and nucleic acid synthesis. The relative impairment varies, as does the tolerable degree of disturbance, which is reflected clinically in the different patterns of liver recovery seen after partial hepatectomy

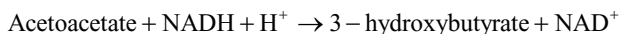


from energy balance may result in metabolic decompensation and organ failure.

A variety of different methods are available with which to gauge hepatic energy balance, and determinations may be performed on peripheral blood or alternatively on the liver itself (by invasive and non-invasive means).

7.4.1 Peripheral Blood Redox State

Hepatic mitochondrial redox state can be estimated by measurement of the relative abundance of ketone bodies in peripheral blood. The ratio of acetoacetate to hydroxybutyrate (the arterial ketone body ratio, AKBR) is in equilibrium with that of oxidized to reduced nicotinamide-adenine dinucleotide (NAD⁺/NADH) in mitochondria [19]:



The balance between these states of NAD reflects the ATP synthesizing potential of the mitochondria. When electron acceptor (oxygen) availability is limited the ratio of NAD⁺/NADH falls, ATP generation is reduced and energy state declines: these changes are also reflected in a decrease acetoacetate/hydroxybutyrate ratio (and for biochemically analogous reasoning a decrease in the pyruvate to lactate ratio).

In the liver, acetoacetate is produced via the formation of 3-hydroxy-3-methylglutaryl-CoA (HMGCoA) and also by the deacylase reaction from acetoacetyl-CoA; when conditions leading to accumulation of reducing equivalents prevail, conversion to hydroxybutyrate increases.

The liver is the predominant source of ketone bodies, although other tissues are involved in their subsequent metabolism. The ratio of acetoacetate to hydroxybutyrate in arterial blood has been shown to be related to hepatic

mitochondrial redox state [20]. A fall in arterial ketone body ratio can be taken to represent a decline in hepatic mitochondrial redox (phosphorylating) potential, and hence attenuation of those aspects of liver function that are dependent on energy supply. Single pre-operative measures of arterial ketone body ratio are of limited use in predicting outcomes, although refinements based on dynamic response to glucose loading have been described (see below) [21]. Serial post-operative estimates of arterial ketone body ratio can identify individuals most likely to develop hepatic failure after liver resection [22].

7.4.2 Tissue Adenine Nucleotide and Mitochondrial Analysis

Because of the requirement for tissue biopsy these measurements have principally been used in a research setting. Nevertheless, the information has proved valuable for proof of concept of novel, non-invasive methods for estimating energy state (see below). Assays of tissue-level metabolism are often based on chemical analysis of biopsy specimens for high-energy phosphate compounds. The relative concentrations of adenosine mono-phosphate (AMP), adenosine di-phosphate (ADP) and adenosine tri-phosphate (ATP) are used to determine the cellular energy charge (or equivalently the phosphorylation potential). As discussed earlier, these parameters are central to regulation of metabolism by constraining the balance between energy-producing and energy-consuming reactions. Alternative techniques involve analysis of mitochondrial phosphorylative activity and cytochrome chain component redox state. In general, the diseased liver (whether by dint of biliary obstruction or parenchymal pathology) displays altered energy-chain activity with negative influence on ATP-synthesizing

ability: these findings are predictive of complications after liver resection as a consequence of decreased functional reserve [23–25].

7.4.3 Magnetic Resonance Spectroscopy

Spectroscopy describes the interaction of electromagnetic radiation with matter, and in this context the resonant exchange of energy by nuclei in a magnetic field. This is an emerging technique which allows non-invasive assay of hepatic intracellular metabolism in vivo. The measurements can be performed on standard magnetic resonance imaging (MRI) systems after suitable adaptation, and are increasingly being used in the modern clinical arena. The basis of the technique is similar to that of the more familiar magnetic resonance (hydrogen nucleus) imaging except that the information is obtained from a different chemical nucleus (usually 31-phosphorus, but also 13-carbon and 23-sodium amongst others). The principle of the measurement is that atomic nuclei have electrical charge and spin, and hence a magnetic moment (by Faraday's laws). If a sample of the tissue to be studied (or indeed a whole organ in vivo) is placed within an external magnetic field, nuclei with odd-quantum spin numbers will align themselves in one of a number of possible quantum states with a slight preponderance of nuclei aligned along the field (low-energy state) according to the Boltzman constant. Within this field, the nuclei precess at a specific rotational rate, the Larmor frequency (analogous to the way in which a spinning gyroscope precesses in the earth's magnetic field). When a radiowave pulse oscillating at the same (Larmor) frequency is applied perpendicular to the original field, the nuclei will absorb energy (the resonance condition) and change their quantum state: a greater proportion are now in the higher energy condition, which can be measured by electromagnetic induction of current in a detector. Different nuclei can be assayed by varying the frequency of the radiowave probing pulse. The signal obtained is mathematically treated (Fourier transformation) to produce a spectrum of concentration against frequency, with nuclei of the same type but within different chemical species, being resolved.

A typical liver spectrum obtained by resonating on the 31-phosphorus nucleus (31-phosphorus magnetic resonance spectroscopy, 31P-MRS) using a 1.5 T clinical MRI system is shown in Fig. 7.3 31-phosphorus magnetic resonance spectroscopy is particularly appealing for the study of liver metabolism in vivo, because this naturally occurring phosphorus isotope is central to biological energy transduction and ubiquitous in cell membrane phospholipids. Using 31-phosphorus magnetic resonance spectroscopy it is possible to measure the energy state of the liver and to appreciate changes in cell membrane composition.

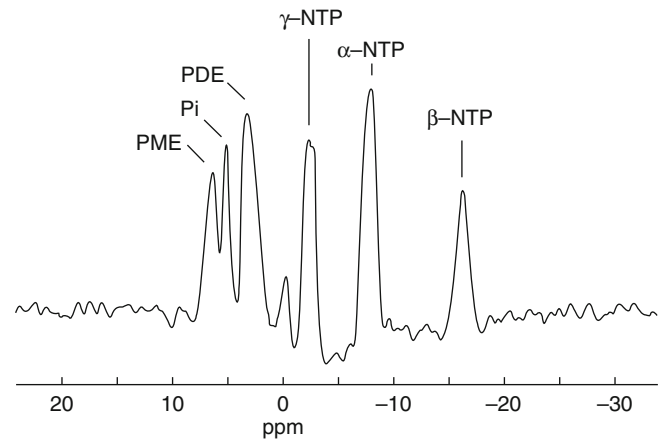
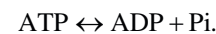


Fig. 7.3 31-phosphorus magnetic resonance spectrum of human liver. Peak area is proportional to amount of metabolite. Peaks labeled on scan: *PME* phosphomonoesters (mainly phospholipids precursors and sugar phosphates), *Pi* inorganic phosphate (product of adenosine triphosphate hydrolysis, which yields adenosine diphosphate and inorganic phosphate: $ATP \leftrightarrow ADP + Pi$), *PDE* phosphodiester (principally phospholipid catabolites with some contribution from cell membranes), and γ -, α -, β -phosphates of nucleotide triphosphates, *NTP* (high-energy phosphate compounds). By convention, the $[\beta\text{-P}]$ NTP peak is taken practically to represent adenosine triphosphate, ATP. Unlabeled peak at zero parts per million (ppm), is phosphocreatine contamination from muscle. Data are conventionally presented as ratios of peak areas, comprising energy status (ATP/*Pi*) and phosphoester metabolites (PME/*PDE*) respectively. Alternatively, individual peak areas may be expressed as a function of total visible phosphate (TP). These measures are independent of the volume of liver from which the signals are obtained

With respect to hepatic energy balance, two relevant phosphate-compounds are assayed: ATP and its hydrolytic breakdown product inorganic phosphate (*Pi*)



The ratio of ATP/*Pi* is an estimate of energy state, analogous to cellular energy charge or phosphorylation potential [26]. Clinical 31P-MRS studies have shown, in general, that in the steady state condition, liver energy balance is often preserved in compensated parenchymal disease [27]. However, under conditions of changing metabolic stress, fluctuations in energy state can be detected. For example, serial measurements of ATP/*Pi* in the regenerating human liver after partial hepatectomy have revealed patterns of high-energy phosphate depletion and recovery [28]. In the clinical setting of obstructive jaundice, biliary decompression has been shown to enhance liver energy status as measured by this technique, a finding which may guide the selection and optimum timing of therapy [29]. This is important because the risks of liver resection are greater when biliary obstruction is present since this is associated with deficient regeneration [2].

The relative proportions of phospholipid compounds detectable by 31-phosphorus magnetic resonance

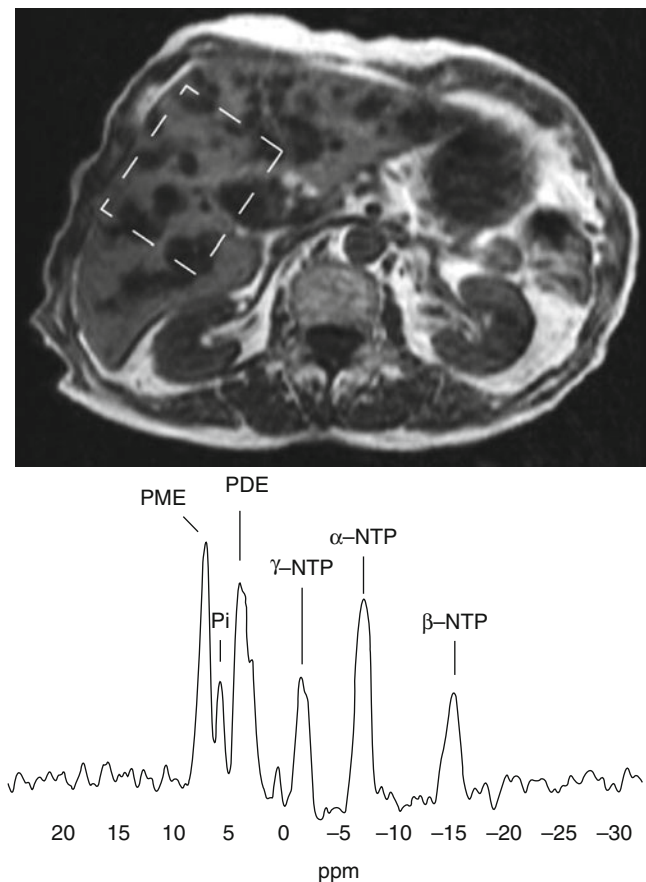


Fig. 7.4 MRI of liver from a patient with obstructive jaundice due to hilar cholangiocarcinoma showing grossly dilated intrahepatic biliary system. The corresponding 31 phosphorus magnetic resonance spectrum is shown. There are readily visible differences in the relative amounts of phospholipids in the PME (phospholipid precursor) and PDE (phospholipid catabolite) peaks when compared to the spectrum from normal liver shown in Fig. 7.3

spectroscopy are reflective of hepatocyte membrane phospholipid composition and metabolism. Two broad peaks representing phospholipids metabolites are generally observed. The phosphomonoester (PME) peak mainly consists of phospholipids precursors, while the phosphodiester peak (PDE) comprises phospholipid catabolites. Changes in the relative abundance of these compounds characterized by a relative excess of phospholipid precursors with respect to catabolites have been interpreted to reflect redirection of phospholipid turnover with generation of secondary messengers and sometimes true amplification of membrane synthesis. In the human liver this pattern of change has been observed in neoplasia, in the maturing neonatal organ, in benign parenchymal disease (including cirrhosis and hepatitis) and in biliary obstruction [27, 29–31]. Figure 7.4 shows a clinical 31 -P magnetic resonance spectrum illustrating membrane phospholipid alterations in a patient with obstructive jaundice due to hilar cholangiocarcinoma. In general, disturbance of phospholipid balance correlates with grade of parenchymal

disease in hepatic fibrosis and cirrhosis and it is likely that such measurements will find a role in the assessment of hepatic status in the future [32]. Changes in hepatic membrane phospholipid composition can also be detected after non-hepatic surgery, and in this context the changes appear to represent biochemical alterations during hepatocyte activation and acute phase physiology [28].

An appealing feature of magnetic resonance spectroscopy is that it can be used serially in the clinical setting to monitor *in vivo* liver function non-invasively, in addition to providing conventional imaging information on hepatic volume recovery, vessel patency and biliary tract morphology (see Sect. 7.6 Longitudinal Evaluation After Hepatectomy).

7.5 Dynamic Tests

These tests generally examine one or more aspects of liver physiology in a time dependent manner or in response to some provocation such a metabolic stress. The advantage of these assessments is that they can quantify hepatic function and when repeated can be used to assess changes in functional status over time. Traditionally, the commonest techniques are tracer excretion studies (clearance tests), although metabolic and bioenergetic measurements and sophisticated nuclear medicine studies are also available to the clinician. The response to portal vein embolization may be considered as a special case of dynamic testing of hepatic functional reserve.

7.5.1 Clearance Tests

These estimate hepatic extraction, handling and excretion of test substances. Depending on the compound selected, the process examined is variably specific but generally reflects the number of hepatocytes (liver cell mass), the functional ability of those hepatocytes and, for very high efficiency elimination, some dependence on hepatic blood flow. The most commonly used are the indocyanine green (ICG) test which measures an energy-dependent transport mechanism, and the aminopyrine test which is reflective of microsomal function. Some tests of metabolic function consequent upon sugar handling, such as galactose elimination capacity, are of practical and theoretical interest.

7.5.1.1 Indocyanine Green Test

This is probably the commonest quantitative liver function test in clinical use. Indocyanine green (ICG) is a tricarbocyanine green coloured dye, which when administered into the circulation rapidly combines with plasma proteins (albumin, lipo-proteins, etc.) and the volume of distribution is therefore the blood volume. ICG is taken up selectively by the liver,

and is excreted unaltered into the bile by an energy (ATP) dependent carrier mediated mechanism. The carrier is a member of the canalicular multiple organic anion transporter (cMOAT) group, which is also responsible for the excretion of bilirubin. The disappearance of ICG from the blood is therefore a measure of an energy-dependant process. ICG exhibits a maximum absorbance at wavelength of 805 nm (near infrared region of the electromagnetic spectrum) and the principle of the measurement is one of photoabsorbance, using pulse densitometry based on pulse oximetry. The test is usually performed by administering ICG intravenously in a dose of 0.5 ml per kg, and monitoring the blood concentration by means of a non-invasive transcutaneous probe (with diodes emitting in the near infrared 805 and 905 nm wavelength) and photocell sensor. Since 805 nm also comprises an isobestic point at which absorption of oxyhaemoglobin intersects with that of deoxyhaemoglobin, the measurement of ICG is independent of oxygen saturation of the blood. ICG distributes uniformly in the blood within 2–3 min after intravascular injection, and the blood level then falls exponentially for about 20 min thereafter, by which time about 97 % is excreted. Because the physical nature of clearance is a natural exponential function, the measurements can be mathematically interpreted to produce values for: plasma half-life ($T_{1/2}$), decay and time constants, and hence plasma disappearance rate and derived retention rate.

The exponential decay function of ICG concentration is converted by logarithmic transformation into a straight line to derive a half-life and decay constant (or its inverse, the time constant). The plasma disappearance rate (PDR, which equates to the decay constant of units 1/time) of the dye in the plasma is calculated from: $PDR = \ln 2 / T_{1/2} * 100 = 0.693 / T_{1/2} * 100$ and expressed as %/min with normal range between 18 and 25. ICG retention value is conventionally measured after 15 min (ICGR15) and is calculated by measurement of the plasma concentration after 15 min expressed as a ratio of that at time zero (calculated by backwards extrapolation of the transformed decay curve) according to the formula: $ICGR15 = [ICG t = 15 \text{ min}] / [ICG t = 0] * 100 (\%)$, with normal range of the order of 0–10 %. An example of a typical ICG clearance test elimination curve is shown in Fig. 7.5.

The ICG test has been shown to be of value in predicting the risk of liver failure and death after hepatic resectional surgery, and is of particular value in patients with liver disease [33, 34]. Discriminant function analysis has shown that an ICG 15 min retention value of 14 % to be a useful predictor of risk, conferring a relative risk of three fold for mortality [35]. Refinements in the estimation of the extent of tolerable parenchymal resection can be made on the basis of ICG testing [36]. ICG testing can be combined with volumetric assessment of parenchymal hepatic resection rate (PHRR, given by Okamoto's formula: $PHRR = \text{resected}$

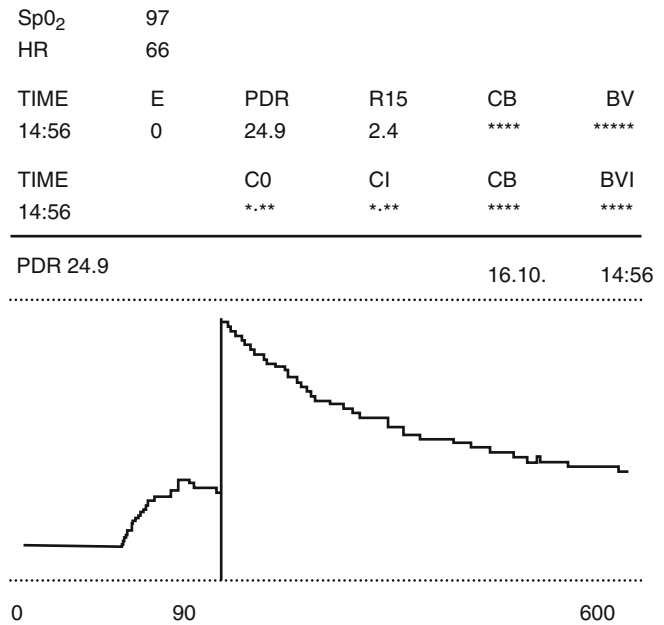


Fig. 7.5 Indocyanine green (ICG) elimination curve in a human subject. The graph shows an exponential decay curve. The derived values are for plasma disappearance rate (PDR)=24.9 %/min and retention value at 15 min (R15)=2.4 %

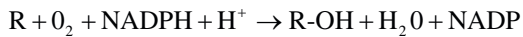
volume–tumor volume/liver volume–tumor volume), and patient age, to produce a predictive score for the likelihood of developing liver failure after hepatectomy [13, 16]. ICG clearance estimation of the future liver remnant has been validated in predicting outcome after resection for biliary cancer [37]. Combined volumetric and functional evaluations of this type have the potential to reduce deaths related to excessive resection in individuals with impaired liver function. Postoperative (remnant liver) recovery of ICG elimination has also been shown to be predictive of the development of complications [38].

It is relevant to the management of patients with cholangiocarcinoma that plasma clearance of ICG is diminished in obstructive jaundice, and in this context it is preferable to measure plasma ICG after the relief of biliary obstruction [37, 39]. Alternatively, when external biliary drainage has been employed, measurement of ICG excretion in bile may more accurately reflect underlying liver energy state, and has been shown to correlate more closely with hepatic ATP levels than plasma ICG clearance [40]. An interesting area of ongoing research is in the use of near infrared spectroscopy for direct measurement of ICG clearance from hepatic parenchyma [41].

7.5.2 Microsomal Capacity Tests

These evaluations probe the capacity of the microsomal cytochrome P450 system, and are in essence an

assessment of liver cell mass. This system of monooxygenases is responsible for the metabolism of a wide range of xenobiotic (and endobiotic) compounds using enzymatic hydroxylation. For any given compound, R, the reaction catalysed is:



A number of test substances can be used for the purposes of testing liver microsomal function, including aminopyrine, caffeine, lidocaine and the lidocaine metabolite monoethylglycinexylidide (MEGX). A significant limitation of these tests is that the enzyme system is inducible by ethanol and influenced by many commonly used drugs, e.g. phenytoin (inductive potentiation) and omeprazole (inhibition).

7.5.2.1 Aminopyrine

The aminopyrine (dimethyl aminoantipyrine) test is the most commonly used, since the progress of metabolic conversion (N-demethylation) can be measured after oral administration by a breath test. The principle of the assay is that a dose of aminopyrine with radioactive (^{14}C) or stable heavy isotope (^{13}C) labelled methyl groups is given. The labelled methyl groups are cleaved by the hydrolytic action of microsomal P450, and subsequently converted to labelled carbon dioxide which is exhaled. The breath may then be analysed by radiation counter or isotope ratio mass spectrometry accordingly, and the result is expressed as percentage of the dose expired in a given time. Despite the potential for confounding outlined above, the aminopyrine breath test has been shown to be a sensitive and quantitative indicator of liver dysfunction, with the ability to stratify surgical risk in patients with liver disease [42]. A composite score, the Liver Resection Index (LRI), has been devised which combines aminopyrine breath test (ABT) with volumetric measures of parenchymal hepatic resection rate (PHRR) and tumor to liver volume ratio to formulate a preoperative risk assessment for fatal post-hepatectomy complications $LRI = ABT(\%)*100/PHRR*age(years)*tumour/liver \text{ volume ratio}$ which has a reported sensitivity of 75 %, specificity of 83 % [43].

7.5.2.2 Lidocaine and MEGX

Lidocaine is a commonly used local anaesthetic and antiarrhythmic agent. Lidocaine is metabolised in the liver by the cytochrome P450 pathway, with formation of monoethylglycinexylidide (MEGX). In the setting of chronic liver disease, the hepatic clearance of lidocaine is reduced with prolongation of its half-life. The generation of MEGX (a build-up or positive exponential process) is consequently reduced and it is the determination of this metabolite that forms the quantitative basis of the liver function test. Clinical

studies indicate that this test is of value in assessing the likelihood of development of complications for cirrhotic patients undergoing liver resection [44].

7.5.3 Hexose Sugar Metabolic Capacity

Handling and metabolism of hexose sugars (glucose, galactose and fructose) by the liver involves energy dependent processes. Dynamic liver function tests using galactose and fructose have been described, together with the effect of glucose loading on ketone body ratio.

7.5.3.1 Galactose Elimination Capacity

The rate-limiting step in the metabolism of galactose within the liver is that catalysed by galactokinase which phosphorylates galactose to galactose-1-phosphate. The reaction is an energy dependent one, consuming ATP, and the phosphorylated galactose is then converted to glucose which is then oxidised in the standard way. The test is performed by administering galactose and then monitoring serial blood levels, or alternatively by a breath test which measures conversion of either radioactive ^{14}C or mass spectrometric detection of ^{13}C , in expired carbon dioxide. The test has been shown to predict complications and survival after hepatic resection [45].

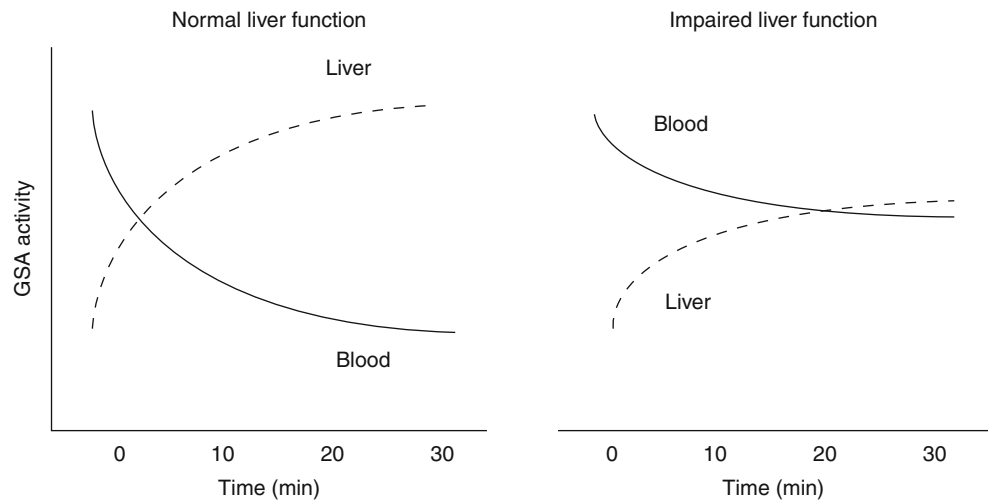
7.5.3.2 Glucose Load: Redox Tolerance Test

The redox tolerance test quantifies the potentiation of hepatic mitochondrial energy metabolism (measured by arterial ketone body ratio, AKBR) in response to an oral glucose loading. The redox tolerance index is derived from the change in ketone body ratio as a function of change in blood glucose level: the lower the index the higher postoperative morbidity and mortality associated with major hepatic resections [21].

7.5.3.3 Fructose Tolerance Test

Fructose is phosphorylated in the liver by fructokinase, a reaction which consumes ATP. A bolus dose of fructose can deplete the liver of inorganic phosphate by trapping within fructose-1-phosphate and thereby limiting the regeneration of ATP from ADP within the cell. These changes can be followed by ^{31}P -phosphorus magnetic resonance spectroscopy which can measure the accumulation of fructose-1-phosphate, depletion of inorganic phosphate and decline in ATP levels [46]. When the liver is diseased, a reduced rate of fructose-1-phosphate formation is found following fructose loading, which may be explained by impaired fructose delivery to, transport into and handling by hepatocytes. These findings are of interest in view of the non-invasive way in which detailed bioenergetic information is obtained. However, the theoretical risk of precipitating lactic acidosis

Fig. 7.6 Schematic ^{99m}Tc -GSA dynamic scintigraphy curves showing disappearance from blood (heart trace) and accumulation in liver. The effect of liver impairment is evidenced by inefficient plasma clearance and hepatic uptake of the tracer



warrants caution in the application of such tests outside of carefully controlled environments.

7.5.4 Hepatobiliary Uptake and Excretion Scintigraphy

7.5.4.1 Iminodiacetic Acid

Isotope-labelled organic anions such as ^{99m}Tc iminodiacetic acid (IDA) permit simultaneous evaluation of total and regional hepatocyte uptake (cell mass estimate) as well as excretory kinetics (functional evaluation). The biliary excretion mechanism is common to that of the energy-dependent organic anion transporter system, and hence the findings of dynamic testing correlate with those of indocyanine green clearance studies [47].

7.5.4.2 Asialoglycoprotein Receptor Scintigraphy

Naturally occurring asialoglycoproteins (ASGP), for example ceruloplasmin, are removed from the circulation by a mechanism that involves adherence to specific receptors in the sinusoidal membrane of hepatocytes (asialoglycoprotein receptor, ASGPR). When the liver is diseased the number of such receptors is reduced which is associated with accumulation of the glycoprotein in the blood. A manufactured scintigraphy agent which binds to ASGPR on hepatocytes, technetium- 99m -galactosyl-human serum albumin (^{99m}Tc -GSA) can be used to probe the dynamics of clearance from blood, hepatic uptake and overall receptor complement. Schematic scintigraphs are shown in Fig. 7.6. Using a radiopharmacokinetic model, hepatic uptake and blood disappearance rates can be measured, and a quantitative index for receptor binding (typically indexed at 15 min) obtained [48, 49]. This value has been shown to be useful for the prediction of liver failure in high-risk patients. The technique is of interest because it is mechanistically distinct from other measures of liver function such as organic anion,

hexose-sugar or microsomal-based clearance tests, and appears to more accurately reflect histological findings. Preoperative regional maximal removal rate of ^{99m}Tc -GSA in the predicted residual liver after hepatectomy has been proposed as a useful test for judging the safety and extent of liver resection [50].

7.5.5 Regenerative Capacity: Portal Vein Embolization

When a tumour is technically suitable for resection but there are concerns about the adequacy of residual hepatic parenchyma (and its functional reserve), one possibility that may be considered is portal vein embolization. Typical indications for portal vein embolization are when predicted remnant liver volume is 25 % or less of total liver volume for normal liver, and 40 % or less when liver function is compromised [51]. The principle of the technique is that when one lobe of the liver is deprived of portal blood flow it undergoes relative atrophy, and a hypertrophic (regenerative) compensatory response is induced within the contra-lateral lobe. In essence this represents a therapeutic trial of regenerative potential: if the hypertrophic response is adequate then formal resectional surgery may be entertained. However if the augmentation of hepatic cell mass is deficient, surgery would likely result in decompensation of an inadequate liver remnant with failure of regeneration. In this sense, the response to portal vein embolization can be considered as a dynamic test of liver function.

The growth of the non-embolized lobe is usually monitored by serial computed tomographic volumetry. In the commonest application, a right portal vein will be embolized to produce left lobe hypertrophy. The average growth of non-embolized tissue that can be anticipated is of the order of 30 %, with mean increase of the order of 10–15 % in total liver volume.

In addition to volumetric measurement (which is a surrogate for liver cell mass), the functional response of the non-embolized lobe can also be assessed. After a successful regenerative response, biliary excretion of indocyanine green by the non-embolized lobe is increased and energy charge is maintained within normal limits [52, 53]. Compensatory accrual of asialoglycoprotein receptor complement can also be monitored in the non-embolized regenerative lobe [54].

7.6 Longitudinal Evaluation After Hepatectomy

An accurate appraisal of liver status is important for the identification of individuals most at risk of developing liver failure after resectional surgery. Recovery from hepatectomy requires a metabolic compromise between differentiated function and parenchymal regrowth, and the likelihood of liver failure ensuing is determined by complex interplay involving liver-specific and general clinical parameters. Liver-specific factors include the current state of liver physiology and reserve, the presence and degree of underlying liver disease (and inherent regenerative potential), the magnitude of parenchymal resection and the size of the remnant liver (and its viability) [1].

Post-operative liver failure has not been uniformly defined, but clinical features include jaundice, ascites, hepatorenal syndrome and onset of encephalopathy. Derangements in commonly used biochemical tests, plasma proteins and coagulation profiles are characteristic, but there is no consensus on when these constitute liver failure, and moreover similar patterns (albeit with less extreme deviations) are noted after liver resection when the recovery proves to be uneventful. Clinical and laboratory experience has shown that events pivoting around the fifth post-operative day are of predictive value for eventual outcome [55, 56]. It is apposite to question what is happening to hepatocytes at this critical time after liver resection, and what types of measurement can inform interpretations and therapeutic decision making.

Preservation of liver function after resection requires that the remaining hepatocytes meet the inherited demands of baseline-differentiated activity. The average cellular workload will however be increased in direct proportion to the number of liver cells lost. Moreover, the remnant liver is also required to host an acute phase reaction characterized by a major redirection of protein synthesis designed to restore bodily equilibrium. The metabolic burden on hepatocytes is increased further by widespread mitosis to replenish lost cell mass. Indirect measures of cell cycling in humans have confirmed the regenerative process to be maximal 4–5 days after hepatectomy [57].

At the hepatocyte level, the metabolic kinetics underlying these events can be studied in a number of direct and indirect

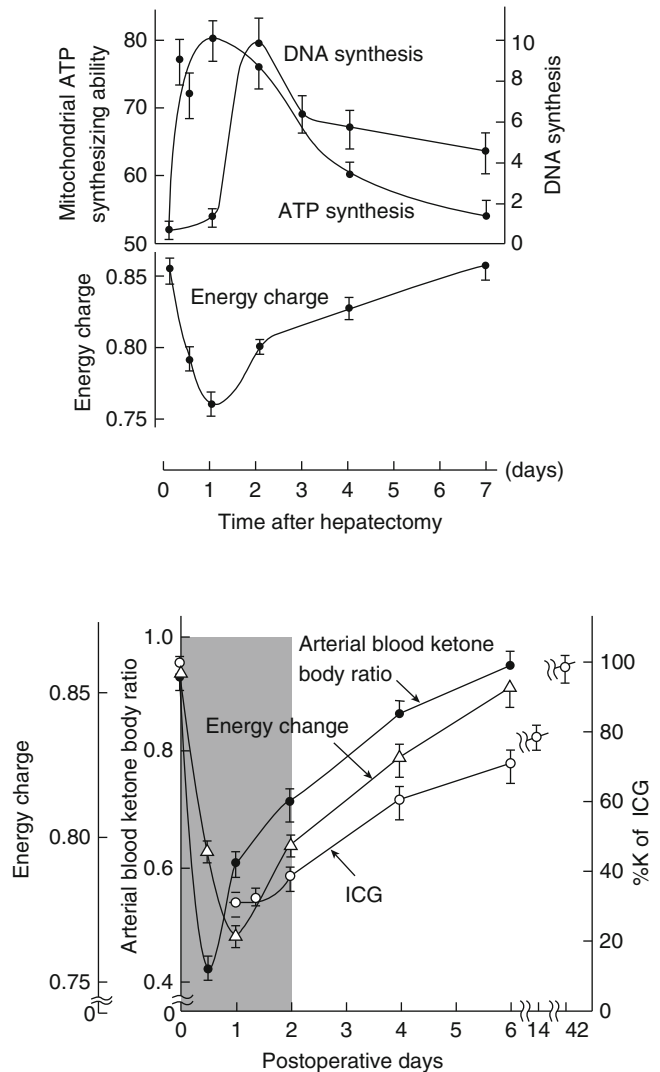


Fig. 7.7 Serial changes in ATP production, energy charge, DNA synthesis, ketone body ratio and ICG clearance after hepatectomy (Adapted and reproduced after Ozawa [62])

ways according to the techniques discussed earlier. Liver regeneration following hepatic resection is associated with a decline in cellular energy charge (with a compensatory increase in net hepatocyte ATP production) which produces a fall in both ketone body ratio and ICG clearance, and these changes normalise when volume recovery is complete [20, 58–61]. Figure 7.7 illustrates the time course of these events. Development of liver failure is reflected in increasing derangements of metabolic indices and can be shown by serial measurement of ketone body ratio and ICG elimination rates [22, 63].

In the modern clinical arena, 31-P MRS can be used for the non-invasive study of hepatic metabolism and regeneration after liver resection [28]. In one such study, the Fig. 7.8 shows that in the remnant normal liver, metabolic balance appears to be initially achieved by diverting energy away

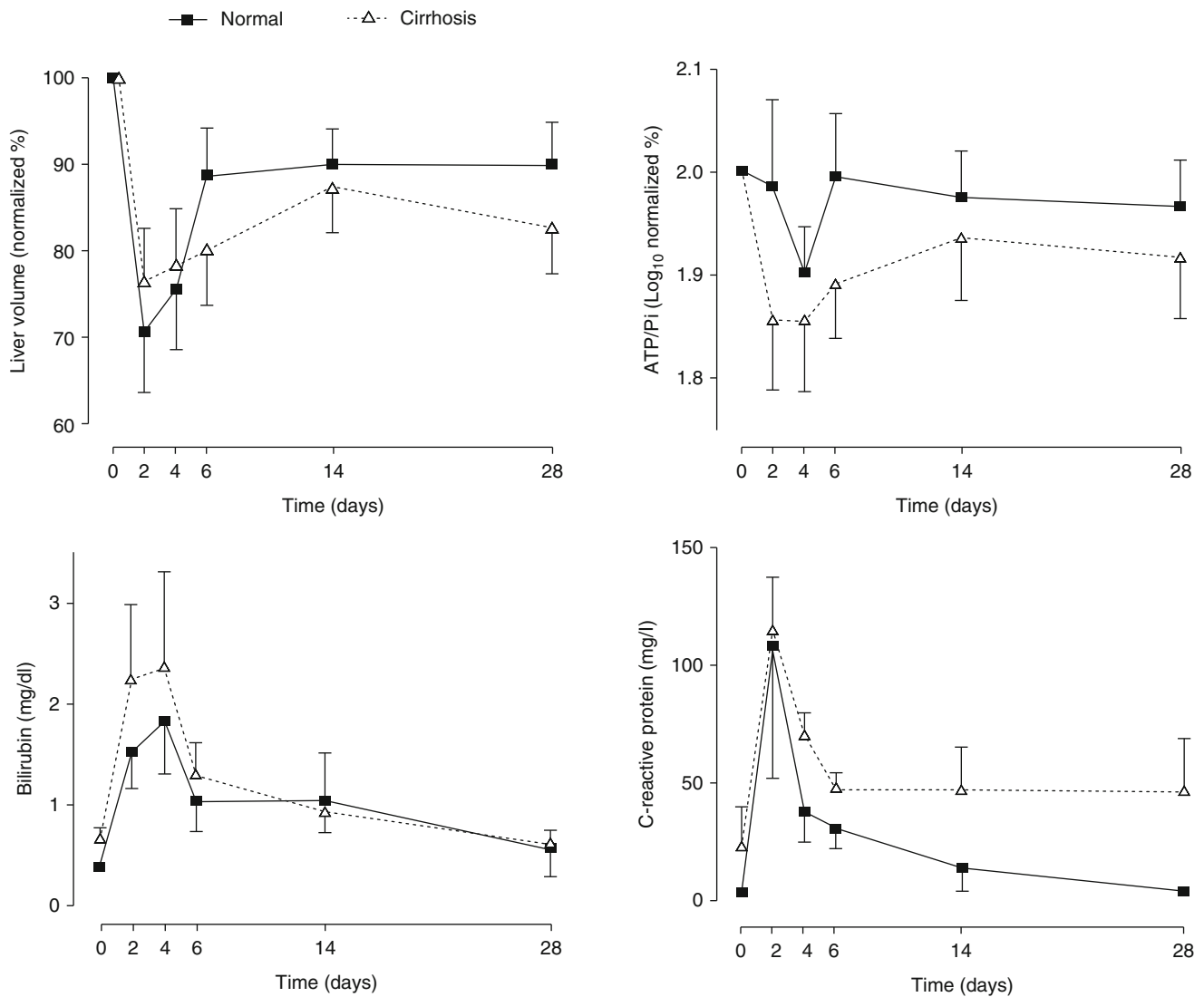


Fig. 7.8 Changes in liver volume (by MRI), energy state (ATP/Pi by ^{31}P MRS), function (bilirubin level) and acute phase reaction (C-reactive protein) after liver resection; comparison of normal and cirrhotic livers (data are mean \pm SE; $n=9$ in each group) (Reproduced after Mann et al.)

from quiescent hepatic functions (such as bilirubin excretion) whilst also rechanneling resources for acute phase requirements. During the maximal growth phase between the fourth and sixth days after hepatectomy, energy expenditure exceeds ATP availability, inducing a decline in energy state. Accordingly, derangements in differentiated function tend to reach their extremes at this time when energy charge is at its nadir, around the fourth post-operative day. As organ regrowth progresses, the distribution of cellular metabolic load becomes more equitable so that energy balance and organ function are restored. This pattern of recovery is disturbed when the liver is diseased. In the cirrhotic liver the early demands of inherited workload and stress reaction are not matched by compensatory changes in energy usage and supply, and a sustained fall in energy state occurs, evident in greater degree of dysfunction. The regenerative response is

retarded (most volume regain occurring between the sixth and fourteenth days) and incomplete, because the depressed energy state restricts protein and nucleic acid synthesis.

How can these findings explain the mechanisms of metabolic control and maintenance of hepatic function during liver regeneration, and can they be used to predict the development of post-resectional liver failure? A useful analogy here is the concept of a liver energy economy, which is comprised of the sum and distribution of reactions for energy-generation and energy-consumption. The metabolic demands on the remaining hepatocytes after liver resection can be apportioned into three vectors: (a) maintenance of differentiated function; (b) acute phase reaction and (c) cellular regeneration. These synchronous competing factors can be combined to produce a representation of hepatic energy economy after partial hepatectomy (Fig. 7.9). Successful

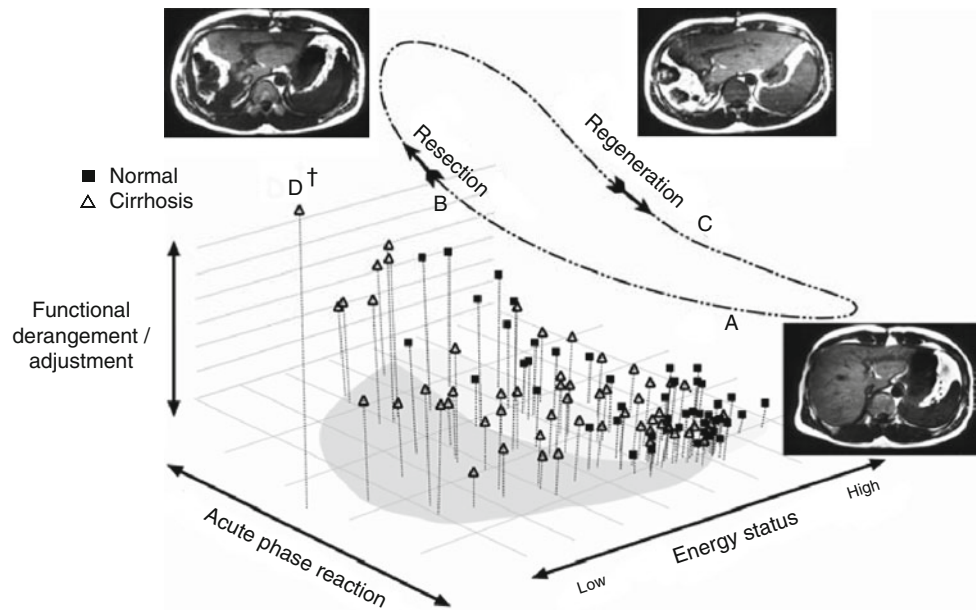


Fig. 7.9 Hepatic energy economy after partial hepatectomy. Three dimensional plot for patients undergoing hepatectomy with normal and cirrhotic livers. *A* Starting conditions. *B* Resection: liver cell mass is lost and acute phase reaction (x-axis) is initiated; DNA synthesis in preparation for mitosis follows. This condition is associated with a fall in energy state (z-axis) and compensatory adjustment (permissible derangement) in differentiated function (which for example could be prothrombin time prolongation on the y-axis). *C* Regeneration: recovery of liver cell mass and restitution of energy balance and functional

status occurs within the framework of the integrated response loop shown here for survivors. The trajectory coordinates for cirrhotic liver (*darker shading*) are more extreme, indicating greater departure from equilibrium and strain on homeostatic recovery mechanisms when the organ is diseased. *D* Departure of an individual from these physiologic boundaries, as a result of inadequate energy production, will result in decompensation of liver function and failure of the organ. This is evident from the coordinates of a patient who died of post-operative liver failure

regeneration of human liver after partial hepatectomy involves modulation of hepatic energy economy in response to changing work demands. The efficiency of this process is influenced by the histopathologic state of the organ, and in turn governs physiologic reserve. Functional derangements after hepatectomy can therefore be regarded as adjustments according to energy status: these may occur within permitted limits, but if energy deficit is excessive then progression to liver failure ensues. The mechanism and timing of post-hepatectomy liver failure can be conceptually explained by an inability to maintain organ energy balance during recovery. This concept can also account for the well known clinical phenomenon of post-operative sepsis precipitating liver failure after hepatectomy [16]. In this instance, the infection induces a second-hit acute phase stress on the liver, which if it occurs at or around the critical regenerative growth spurt may be sufficient to induce metabolic decompensation. This framework can also be used to interpret the therapeutic role of portal vein embolization: in this case, the metabolic burden of regeneration is selectively dissociated from the demands of acute phase reaction, allowing a temporal separation (staging) of the metabolic load such that a critical threshold of energy-balance is not exceeded, and thereby stewarding successful recovery [64]. Pre-growing the remnant liver levers bioenergetic advantage over postoperative

regrowth. With these insights in mind, organ monitoring based on intracellular metabolism after hepatectomy has the potential to provide for the early detection of impending liver failure, and has potential to guide the development and application of novel hepatic support strategies [65].

7.7 Summary and Synthesis

In general, clinical evaluation and standard liver blood tests, combined in a clinico-laboratory scoring system (usually Child-Pugh), provide a reliable means of gauging hepatic function and its reserve. Despite the biologic complexity of liver function, clinicians are able to identify healthy status and to discriminate between well-, moderately- and poorly-compensated liver disease with considerable accuracy using this assessment. Additional testing is usually performed when liver function is judged borderline (or potentially so), or when a major resection is under consideration in an otherwise apparently normal liver. The most useful supportive information is derived from computed tomography volumetric estimation of the anticipated magnitude of loss of hepatocyte cell mass and the size of the liver remnant. Dynamic testing of some component of performance such as substance-clearance (most popularly ICG) or receptor uptake

(commonly by asialoglycoprotein scintigraphy) can augment the volumetric analysis by adding a quantitative functional dimension. In this way the stratification of risk and selection and timing of therapeutic options can be increasingly refined. When functional reserve is judged insufficient to permit liver resection, and this would otherwise be the preferred course of action, then in suitable instances a therapeutic trial of portal vein embolization may be performed. Emerging technologies that measure organ-specific metabolism non-invasively such as magnetic resonance spectroscopy are poised to play an increasingly important role in the evaluation of liver function in the future.

References

1. Yamanaka N, Okamoto E, Kawamura E, et al. Dynamics of normal and injured human liver regeneration after hepatectomy as assessed on the basis of computed tomography and liver function. *Hepatology*. 1993;18:79–85.
2. Yokoyama Y, Nagino M, Nimura Y. Mechanism of impaired hepatic regeneration in cholestatic liver. *J Hepatobiliary Pancreat Surg*. 2007;14:159–66.
3. Schroeder R, Marroquin C, Bute B, et al. Predictive indices of morbidity and mortality after liver resection. *Ann Surg*. 2006;243:373–9.
4. Sitzmann J, Greene P. Perioperative predictors of morbidity following hepatic resection for neoplasm. *Ann Surg*. 1994;219:13–7.
5. Noun R, Jagot P, Farges O, et al. High preoperative serum alanine transferase levels: effect on the risk of liver resection in child grade A cirrhotic patients. *World J Surg*. 1997;21:390–5.
6. Didolkar M, Fitzpatrick L, Elias G, et al. Risk factors before hepatectomy, hepatic function after hepatectomy and computed tomographic changes as indicators of mortality from hepatic failure. *Surg Gynecol Obstet*. 1989;169:17–26.
7. Pugh R, Murray-Lyon I, Dawson J, et al. Transection of the oesophagus for bleeding oesophageal varices. *Br J Surg*. 1973;60:646–9.
8. Franco D, Capussotti L, Smadja C, et al. Resection of hepatocellular carcinomas. *Gastroenterology*. 1990;98:733–8.
9. Nonami T, Harada A, Kurokawa T, et al. Hepatic resection for hepatocellular carcinoma. *Am J Surg*. 1997;173:288–91.
10. Vauthey J, Klimstra D, Franceschi D, et al. Factors affecting long-term outcome after hepatic resection for hepatocellular carcinoma. *Am J Surg*. 1995;169:28–35.
11. Freeman R, Wiesner R, Roberts J, et al. Improving liver allocation: MELD and PELD. *Am J Transplant*. 2004;4:114–31.
12. Cucchetti A, Ercolani G, Vivarelli M, et al. Impact of model for end-stage liver disease (MELD) score on prognosis after hepatectomy for hepatocellular carcinoma on cirrhosis. *Liver Transpl*. 2006;12:966–71.
13. Okamoto E, Kyo A, Yamanaka N, et al. Prediction of the safe limits of hepatectomy by combined volumetric and functional measurements in patients with impaired hepatic function. *Surgery*. 1984;95:586–92.
14. Soyer P, Roche A, Elias D, et al. Hepatic metastases from colorectal cancer: influence of hepatic volumetric analysis on surgical decision making. *Radiology*. 1992;184:695–7.
15. Belghiti J, Ogata S. Assessment of hepatic reserve for the indication of hepatic resection. *J Hepatobiliary Pancreat Surg*. 2005;12:1–3.
16. Yamanaka N, Okamoto E, Oriyama T, et al. A prediction scoring system to select the surgical treatment of liver cancer. *Ann Surg*. 1994;219:342–6.
17. Behrns K, Tsiotos G, Desouza N, et al. Hepatic steatosis as a potential risk factor for major hepatic resection. *J Gastrointest Surg*. 1998;2:292–8.
18. Atkinson D. The energy charge of the adenylate pool as a regulatory parameter: interaction with feedback modifiers. *Biochemistry*. 1968;7:4030–4.
19. Williamson D, Lund P, Krebs H. The redox state of free nicotinamide-adenine dinucleotides in the cytoplasm and mitochondria of rat liver. *Biochem J*. 1967;103:514–27.
20. Ozawa K, Fujimoto T, Nakatani T, et al. Changes in hepatic energy charge, blood ketone body ratio, and indocyanine green clearance in relation to DNA synthesis after hepatectomy. *Life Sci*. 1982;31:647–53.
21. Mori K, Ozawa K, Yamamoto Y, et al. Response of hepatic mitochondrial redox state to oral glucose load: redox tolerance test as a new predictor of surgical risk in hepatectomy. *Ann Surg*. 1990;211:438–46.
22. Kiuchi T, Ozawa K, Yamamoto Y, et al. Changes in arterial ketone body ratio in the phase immediately after hepatectomy: prognostic implications. *Arch Surg*. 1990;125:655–9.
23. Komura M, Chijiwa K, Naito T, et al. Sequential changes of energy charge, lipoperoxide level, and DNA synthesis rate of the liver following biliary obstruction in rats. *J Surg Res*. 1996;61:503–8.
24. Jikko A, Taki Y, Nakamura N, et al. Adenylate energy charge and cytochrome a(+a3) in the cirrhotic rat liver. *J Surg Res*. 1984;37:361–8.
25. Sakai Y, Tanaka A, Ikai I, et al. Cytochrome c oxidase activity in human liver specimens: an index of prognosis for hepatic resection. *Arch Surg*. 1990;125:632–5.
26. Gadian D. Nuclear magnetic resonance and its applications to living systems. Oxford: Clarendon; 1982.
27. Menon D, Sargentoni J, Taylor-Robinson S, et al. Effect of functional grade and etiology on in vivo hepatic phosphorus-31 magnetic resonance spectroscopy in cirrhosis: biochemical basis of spectral appearances. *Hepatology*. 1995;21:417–27.
28. Mann D, Lam W, Hjelm N, et al. Metabolic control patterns in acute phase and regenerating human liver determined in vivo by 31-phosphorus magnetic resonance spectroscopy. *Ann Surg*. 2002;235:408–16.
29. Mann D, Lam W, Hjelm N, et al. Biliary drainage for obstructive jaundice enhances hepatic energy status in humans: a 31-phosphorus magnetic resonance spectroscopy study. *Gut*. 2002;50:118–22.
30. Maris J, Evans A, McLaughlin A, et al. 31P nuclear magnetic resonance spectroscopic investigation of human neuroblastoma in situ. *N Engl J Med*. 1985;312:1500–5.
31. van Wassenaeer-van Hall H, van der Grond J, van Hattum J, et al. 31P magnetic resonance spectroscopy of the liver: correlation with standardized serum, clinical, and histological changes in diffuse liver disease. *Hepatology*. 1995;21:443–9.
32. Jalan R, Sargentoni J, Coutts G, et al. Hepatic phosphorus-31 magnetic resonance spectroscopy in primary biliary cirrhosis and its relation to prognostic models. *Gut*. 1996;39:141–6.
33. Hemming A, Scudamore C, Shackleton C, et al. Indocyanine green clearance as a predictor of successful hepatic resection in cirrhotic patients. *Am J Surg*. 1992;163:515–8.
34. Fan S, Lai C, Lo C, et al. Hospital mortality of major hepatectomy for hepatocellular carcinoma associated with cirrhosis. *Arch Surg*. 1995;130:198–203.
35. Lau H, Man K, Fan S, et al. Evaluation of preoperative hepatic function in patients with hepatocellular carcinoma undergoing hepatectomy. *Br J Surg*. 1997;84:1255–9.
36. Kawasaki S, Makuuchi M, Miyagawa S, et al. Results of hepatic resection for hepatocellular carcinoma. *World J Surg*. 1995;19:31–4.
37. Yokoyama Y, Nishio H, Ebata T, et al. Value of indocyanine green clearance of the future liver remnant in predicting outcome after resection for biliary cancer. *Br J Surg*. 2010;97:1260–8.

38. Matsumata T, Kanematsu T, Yoshida Y, et al. The indocyanine green test enables prediction of postoperative complications after hepatic resection. *World J Surg.* 1987;11:678–81.
39. Stockmann M, Malinowski M, Lock J, et al. Factors influencing the indocyanine green (ICG) test: additional impact of acute cholestasis. *Hepatogastroenterology.* 2009;56:734–8.
40. Chijiwa K, Watanabe M, Nakano K, et al. Biliary indocyanine green excretion as a predictor of hepatic adenosine triphosphate levels in patients with obstructive jaundice. *Am J Surg.* 2000;179:161–6.
41. Jiao L, El-Desoky A, Seifalian A, et al. Effect of liver blood flow and function on hepatic indocyanine green clearance measured directly in a cirrhotic animal model. *Br J Surg.* 2000;87:568–74.
42. Gill R, Goodman M, Golfus G, et al. Aminopyrine breath test predicts surgical risk for patients with liver disease. *Ann Surg.* 1983;198:701–4.
43. Cohnert T, Rau H, Buttler E, et al. Preoperative risk assessment of hepatic resection for malignant disease. *World J Surg.* 1997;21:396–401.
44. Ercolani G, Grazi G, Calliva R, et al. The lidocaine (MEGX) test as an index of hepatic function: its clinical usefulness in liver surgery. *Surgery.* 2000;127:464–71.
45. Redaelli C, Dufour J, Wagner M, et al. Preoperative galactose elimination capacity predicts complications and survival after hepatic resection. *Ann Surg.* 2002;235:77–85.
46. Sakuma H, Itabashi K, Takeda K, et al. Serial P-31 MR spectroscopy after fructose infusion in patients with chronic hepatitis. *J Magn Reson Imaging.* 1991;1:701–4.
47. Bennink R, Dinant S, Erdogan D, et al. Preoperative assessment of postoperative remnant liver function using hepatobiliary scintigraphy. *J Nucl Med.* 2004;45:965–71.
48. Kwon A-H, Ha-Kawa S, Uetsuji S, et al. Preoperative determination of the surgical procedure for hepatectomy using technetium-99m-galactosyl human serum albumin (99mTc-GSA) liver scintigraphy. *Hepatology.* 1997;25:426–9.
49. Satoh K, Yamamoto Y, Nishiyama Y, et al. 99mTc-GSA liver dynamic SPECT for the preoperative assessment of hepatectomy. *Ann Nucl Med.* 2003;17:61–7.
50. Kwon A-H, Matsui Y, Kaibori M, et al. Preoperative regional maximal removal rate of technetium-99m-galactosyl human serum albumin (GSA-Rmax) is useful for judging the safety of hepatic resection. *Surgery.* 2006;140:379–86.
51. Abdalla E, Hicks M, Vauthey J. Portal vein embolization: rationale, technique and future prospects. *Br J Surg.* 2001;88:165–75.
52. Uesaka K, Nimura Y, Nagino M. Changes in hepatic lobar function after right portal vein embolization: an appraisal by biliary indocyanine green excretion. *Ann Surg.* 1996;223:77–83.
53. Chijiwa K, Saiki S, Noshiro H, et al. Effect of preoperative portal vein embolization on liver volume and hepatic energy status of the nonembolized liver lobe in humans. *Eur Surg Res.* 2000;32:94–9.
54. Kubo S, Shiomi S, Tanaka H, et al. Evaluation of the effect of portal vein embolization on liver function by 99mTc-galactosyl human serum albumin scintigraphy. *J Surg Res.* 2002;107:113–8.
55. Balzan S, Belghiti J, Farges O, et al. The “50-50 Criteria” on postoperative day 5: an accurate predictor of liver failure and death after hepatectomy. *Ann Surg.* 2005;242:824–9.
56. Cucchetti A, Ercolani G, Cescon M, et al. Recovery from liver failure after hepatectomy for hepatocellular carcinoma in cirrhosis: meaning of the model for end-stage liver disease. *J Am Coll Surg.* 2006;203:670–6.
57. Francavilla A, Panella C, Polimeno L, et al. Hormonal and enzymatic parameters of hepatic regeneration in patients undergoing major liver resections. *Hepatology.* 1990;12:1134–8.
58. Ove P, Takai S, Umeda T, et al. Adenosine triphosphate in liver after partial hepatectomy and acute stress. *J Biol Chem.* 1967;242:4963–71.
59. Kamiyama Y, Ozawa K, Honjo I. Changes in mitochondrial phosphorylative activity and adenylate energy charge of regenerating rabbit liver. *J Biochem.* 1976;80:875–81.
60. Rikkers L, Moody F. Estimation of functional hepatic mass in resected and regenerating rat liver. *Gastroenterology.* 1974;67:691–9.
61. Okochi O, Kaneko T, Sugimoto H, et al. ICG pulse spectrophotometry for perioperative liver function in hepatectomy. *J Surg Res.* 2002;103:109–13.
62. Ozawa K. Liver surgery approached through the mitochondria. Tokyo: Medical Tribune; 1992.
63. Sugimoto H, Okochi O, Hirota M, et al. Early detection of liver failure after hepatectomy by indocyanine green elimination rate measured by pulse dye-densitometry. *J Hepatobiliary Pancreat Surg.* 2006;13:543–8.
64. Mann D, Lam W, Hjelm N, et al. Human liver regeneration: hepatic energy economy is less efficient when the organ is diseased. *Hepatology.* 2001;34:557–65.
65. Demetriou A, Brown R, Busutil R, et al. Prospective, randomized, multicenter, controlled trial of a bioartificial liver in treating acute liver failure. *Ann Surg.* 2004;239:660–70.